

## 7.0 STUDY 5 - PHANTOM POSITION DEPENDENCE

M. R. Thorson and G.W.R. Endres

### FOREWORD

Sensitivity of the Hanford dosimeter response to its position relative to the phantom and the neutron source has always been recognized. A thorough investigation was performed to quantify dosimeter response according to

- a) dosimeter position on phantom,
- b) dosimeter distance from phantom, and
- c) angular relationship of dosimeter relative to neutron source and phantom.

Results were obtained for neutron irradiation at several different energies.

### SUMMARY

Dependence of HMPD response upon dosimeter angle relative to the phantom and dosimeter position on the phantom adds considerably to the dosimeter inaccuracy and low precision in fast neutron fields. Angular and positional dependence cause the dosimeter to underrespond to fast neutrons by as much as 50% of a given dose equivalent. Other conclusions which can be drawn are as follows

1. Positional dependence is a function of the amount of neutron moderating material immediately behind chips 3 and 4.
2. Positional dependence decreases considerably at high (10 MeV) neutron energies (at 100 keV it is 45% greater than at 10 MeV).
3. Positional dependence of the dosimeter to  $^{252}\text{Cf}$  can be quantified as having a multiplicative standard deviation equal to 3% of TLD chip 3's reading and 8% of TLD chip 4's reading.
4. Attaching a thin moderator to the back of the dosimeter considerably decreases its positional dependence.

5. There is a depression in HMPD calculated fast neutron dose equivalent over the lungs. Values over the lungs are about 30% lower than values in the center chest region. (These values were determined on the Rando phantom.)
6. Sensitivity to fast neutrons decreases 55% when the dosimeter is at an angle of 45° relative to the front plane of the phantom.

## INTRODUCTION

Interest in the performance of the Hanford multipurpose dosimeter (HMPD) in field exposures involving neutron radiation has increased considerably in the past few years. The possibility that quality factors may be increased for fast neutrons and that the HMPD may be used for field exposures not considered in its initial design are two of the principle reasons for this interest. Since it was shown in previous years that the positioning of the dosimeter affected its response, we decided it was important to evaluate the dosimeter's positional dependence for several energies of neutrons.

The dosimetry technology staff at Pacific Northwest Laboratory (PNL) tested the dosimeter's response to neutrons ranging from 0.025 eV to 16 MeV in energy. These tests were performed on a Rando phantom and were accomplished by numerous exposures with dosimeters placed at various positions in the chest region of the phantom. Also dosimeters were exposed at various angles and distances relative to the phantom.

## RECOMMENDATIONS

The major recommendation which can be made from this study is that as long as an albedo dosimeter such as the HMPD is used to measure fast neutron dose equivalent, an attempt should be made to standardize the moderator behind the dosimeter. This could be accomplished by attaching a thin, perhaps 1/4-inch, moderator to the back of the dosimeter and having the dosimeter attached flat against the body in a standardized wearing position.

## CONCEPT OF POSITIONAL DEPENDENCE, ANGLE DEPENDENCE AND DISTANCE DEPENDENCE OF NEUTRON RESPONSES

Positional dependence, as described in this report, is the dependence of HMPD response upon the physical part of the phantom or person to which it is attached. This should be contrasted to angular dependence, which is the dependence of HMPD response upon the angle between the plane of the dosimeter and the plane of the phantom, and distance dependence, which is the dependence of the HMPD response upon the distance between the dosimeter and the phantom. In this study, only dependence to neutron irradiations--primarily fast neutron irradiations--were examined.

### POSITIONAL DEPENDENCE TO A $^{252}\text{Cf}$ SPECTRUM

Bare Californium-252 was used as the primary source of fast neutrons because it was readily available and was the standard fast neutron source used in calibrating the dosimeters. Its average neutron energy is 2.3 MeV. The spectrum, as shown in Appendix A, is a smooth spectrum with a median energy of 0.8 MeV.

To measure the positional dependence, the five chip HMPD with two TLD chips behind each filter was used. The five chip dosimeter was used in preference to the standard four chip dosimeter in order to better describe neutron dependence without confusing it with problems from inadequate gamma correction of the four chip dosimeter.

The phantoms used were the water jug and the Rando phantom. The water jug phantom is elliptical in horizontal cross section (11-5/8 inch x 7-7/8 inch), 15-3/4 inches high, and filled with tapwater. The Rando phantom is a composite of low- and high-density polyethylene and bone, shaped into the figure of a man. It is approximately equivalent to a "standard man" missing only legs and arms. The Rando phantom is shown in Figure 7.1.

### Evidence for Positional Dependence

The initial evidence for positional dependence came from comparing the HMPD response when placed around the Rando phantom to that when placed around a water jug phantom. For this comparison, dosimeters were attached in a horizontal ring around the thorax region of the Rando phantom, as shown in Figures 7.1a and 7.1b. Similarly, dosimeters were attached in a ring around the water jug phantom. Each phantom was then separately exposed to  $^{252}\text{Cf}$ , one meter directly in front of the phantom. Several days after the exposures, each dosimeter was read out. From this, the fast neutron dose was calculated and is shown in Figures 7.2 and 7.3.

Figure 7.2 shows response of dosimeters placed around the water jug phantom. These responses were corrected for distance from the source, so they are all relative to one meter. The given dose equivalent was 1000 mrem at the front of the phantom. Note that the thermoluminescence of TLD chips 3 and 4<sup>(a)</sup> changes gradually from the front, at  $0^\circ$ , to the back, at  $180^\circ$ . As a result, the calculated fast neutron dose changes gradually from front to back.

In contrast, Figure 7.3 shows the HMPD response when dosimeters were placed in a horizontal ring around the Rando phantom chest and simultaneously exposed to  $^{252}\text{Cf}$ . The exposure was identical to that on the water jug. Note that the thermoluminescence of TLD chips 3 and 4 changes more abruptly from the front to the back than on the water jug. As a result, the calculated fast neutron dose changes more abruptly from front to back.

Fluctuations in calculated fast neutron dose in both Figure 7.2 and 7.3 resulted from dependence upon position of the dosimeter on the phantom, angle of the dosimeter relative to the incident radiation and shielding effect of the phantom on dosimeters between  $90$  and  $180^\circ$ . The physical setup was nearly identical for both exposures, and the cross sectional shape of the water jug phantom was a close approximation of that of the Rando phantom chest. Both

---

(a) For the  $^{252}\text{Cf}$  neutron dose equivalent calculations, the dose equivalent was approximately proportional to  $(2R4-R3)$ ; therefore, the thermoluminescent readings of chip 4 (R4) and the readings of chip 3 (R3) were the only important parameters in determining fast neutron dose.

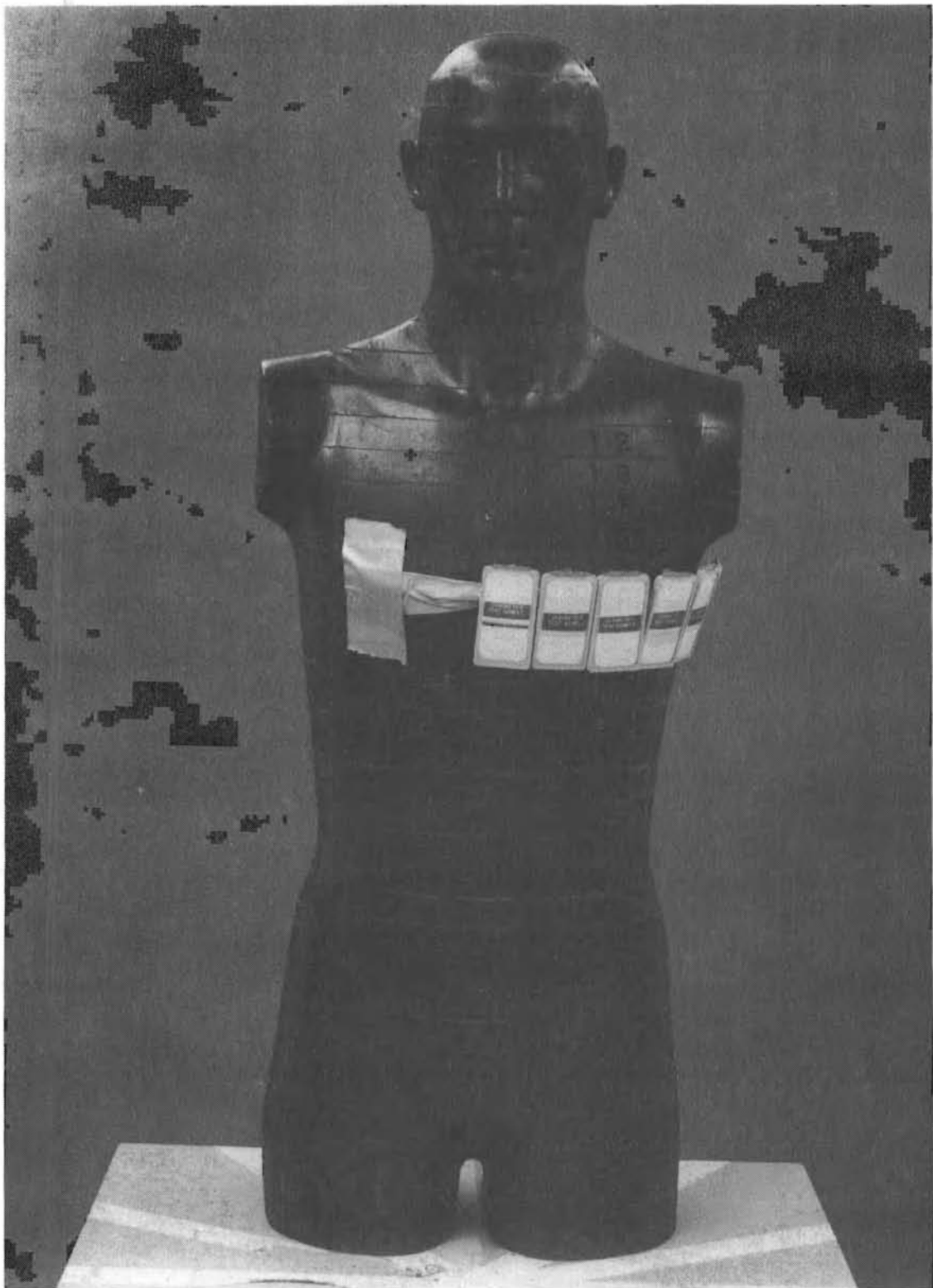


FIGURE 7.1a. Rando Phantom with Dosimeter Placement Around Thorax-  
Anterior

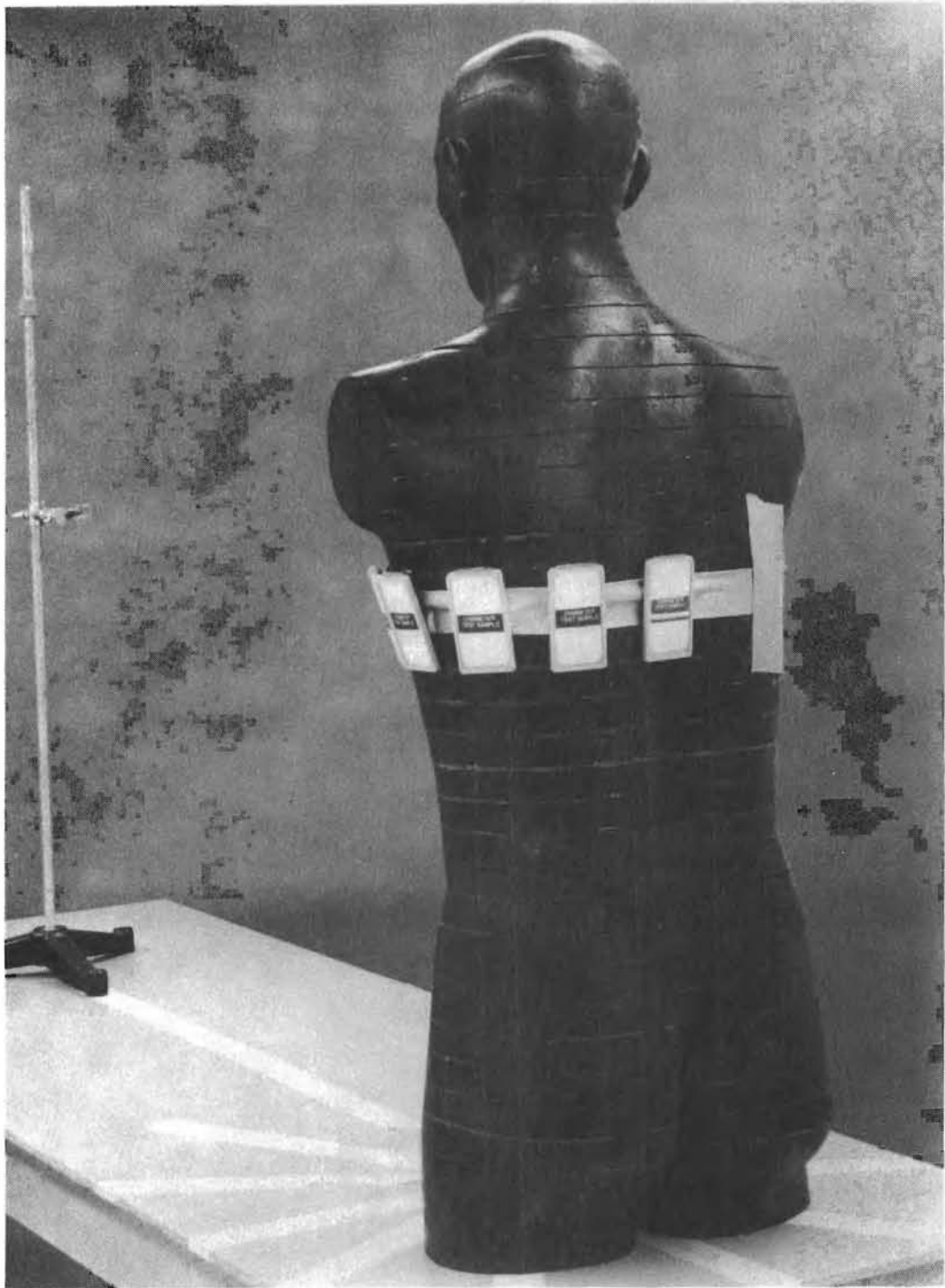


FIGURE 7.1b. Rando Phantom with Dosimeter Placement Around Thorax-  
Posterior

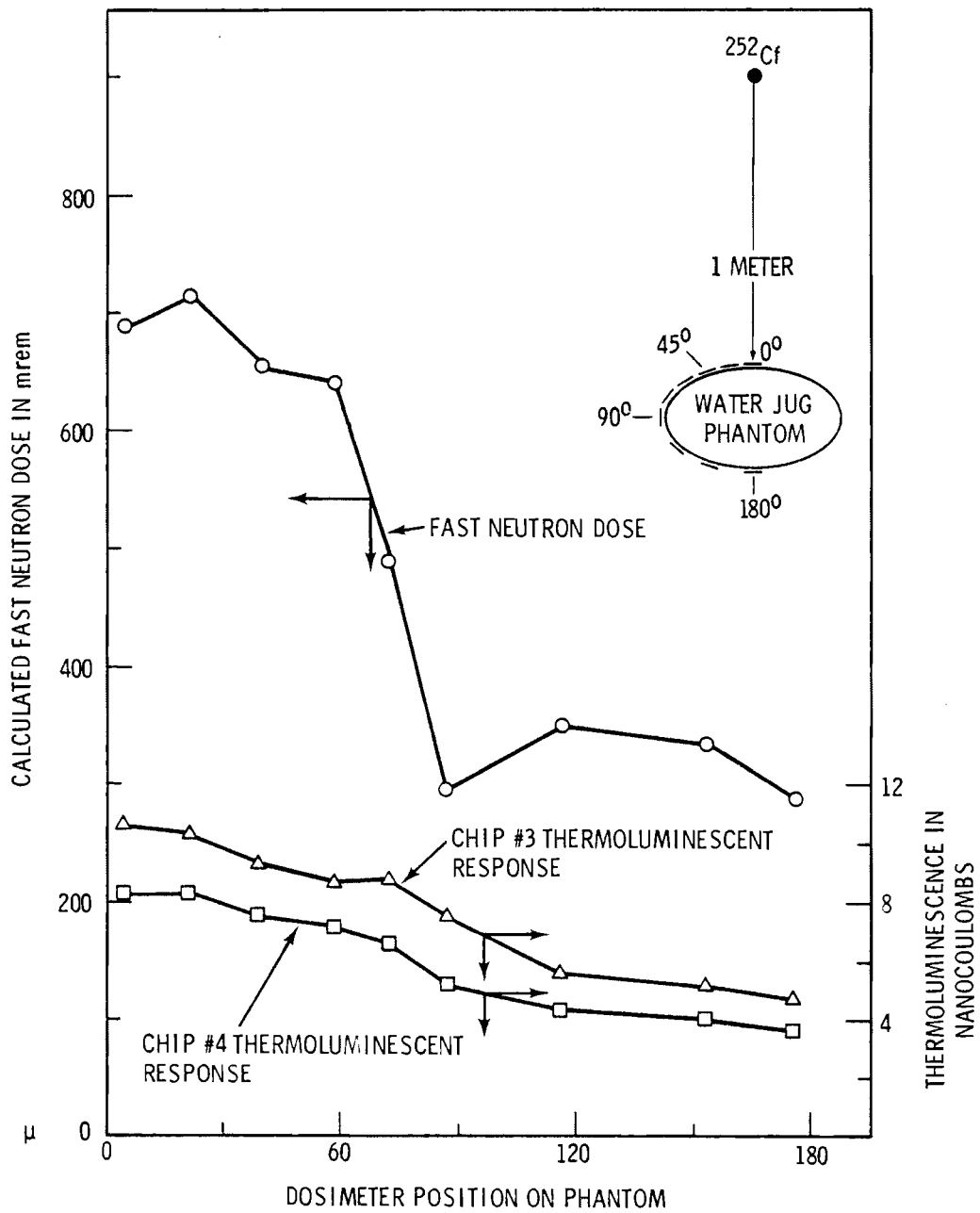
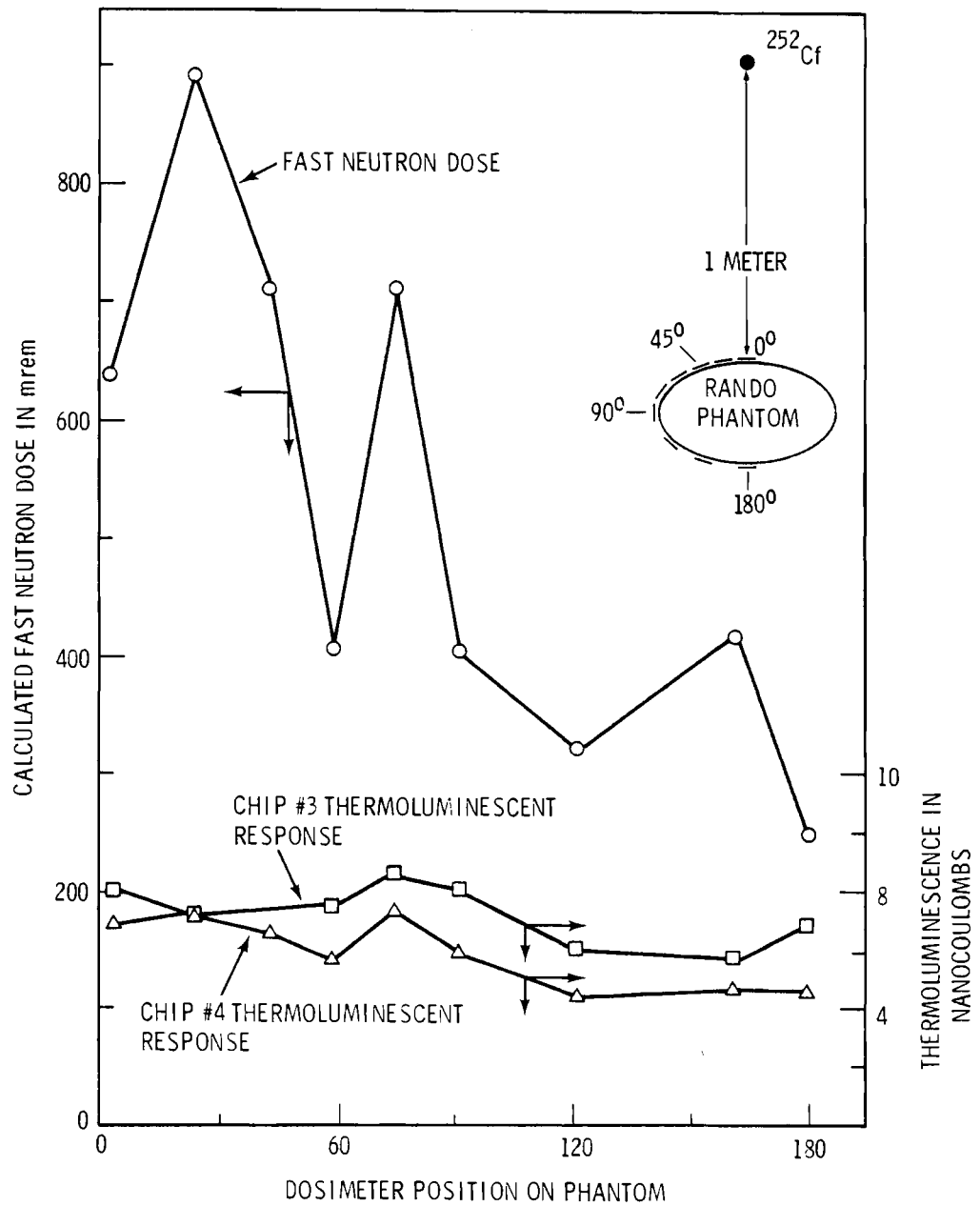


FIGURE 7.2. HMPD Response with Position on the Water Jug Phantom (Dose received is 1000 mrem at front of phantom. All values are corrected to one meter from source.)



**FIGURE 7.3.** HMPD Response with Position on the Rando Phantom. (Dose received is 1000 mrem at front of phantom. All values are corrected to one meter from source.)



exposures had almost identical distance, angle, and shielding between the radiation source and the dosimeters. Therefore, the main source of difference between responses shown in the two figures, was the effect of the different neutron-moderating material behind the dosimeters (i.e., positional dependence).

#### Source of Positional Dependence

Positional dependence is a phenomena which results from the different neutron moderating and absorbing characteristics of material or tissue immediately behind the dosimeter. If the material is of high hydrogen density material (and therefore is a good neutron moderator), it will cause the TLD chip immediately in front of it to "see" more thermal neutrons and therefore store more thermoluminescence than a TLD chip with low hydrogen density material behind it.

In the case of the Rando phantom, the presence of bone, low-density polyethylene and high-density polyethylene in close proximity creates a composite of high- and low-neutron-moderating material. If the dosimeter is moved a few inches on the Rando phantom, its fast neutron response varies considerably. Even the one inch separating chips 3 and 4 causes them to vary somewhat independently of each other. As a result, the relative thermoluminescence of chip 3 compared to chip 4 varies considerably more on the Rando phantom than it does on the water jug phantom.

#### Sources of Thermoluminescence of Chips 3 and 4 on the Rando Phantom

Thermoluminescence of chip 3 in a pure neutron field is due to four main components:

- A. Incident thermal neutrons,
- B. Albedo thermal neutrons which are back-reflected from the phantom (i.e., albedo thermal neutrons originating from incident thermal neutrons),
- C. Epicadmium (above 0.4 ev) neutrons which are captured by the LiF chip, and

D. Epicadmium neutrons which are thermalized by the body, reflected back and captured by the LiF chip.

While chip 3's thermoluminescence is the sum of thermoluminescence from all four components, chip 4's thermoluminescence is the sum of thermoluminescence from only B, C, and D above.<sup>(a)</sup>

The fast neutron dose equation attempts to measure thermoluminescence from components C and D. Roughly, this is done by measuring the ratio of thermoluminescence from component A to that of component B (approximately equal to one).<sup>(b)</sup> Then an equation is used to calculate the sum of thermoluminescence from components C and D. Neglecting the gamma subtraction (R5), this equation is approximately:

$$(2R4-R3) \cdot \text{constant} = \text{fast neutron dose equivalent}$$

This is roughly proportional to:

$$2(B + C + D) - (A + B + C + D)$$

Since  $A \cong B$ ,

$$2 \cdot (B + C + D) - (A + B + C + D) \cong 2 \cdot (B + C + D) - (2 \cdot B + C + D) = C + D$$

In order to determine the cause of fluctuating calculated fast neutron dose and fluctuating thermoluminescence, the components of thermoluminescence for each position on the Rando phantom were determined and are shown in Figure 7.4.<sup>(c)</sup>

---

(a) Actually, the contribution from B is slightly less for chip 4 because of the "shadowing" effect of cadmium.

(b) The value usually used for HMPDs is  $A/B = 1.15$ .

(c) This information was gathered by a specially built dosimeter. Basically it involved several combinations of cadmium and tin designed to eliminate thermal neutrons from selected directions. Using this dosimeter, it was possible to directly measure: A, C and B + D. B was assumed equal to A ( $B = A$ ), and D was calculated by subtracting A from B + D.

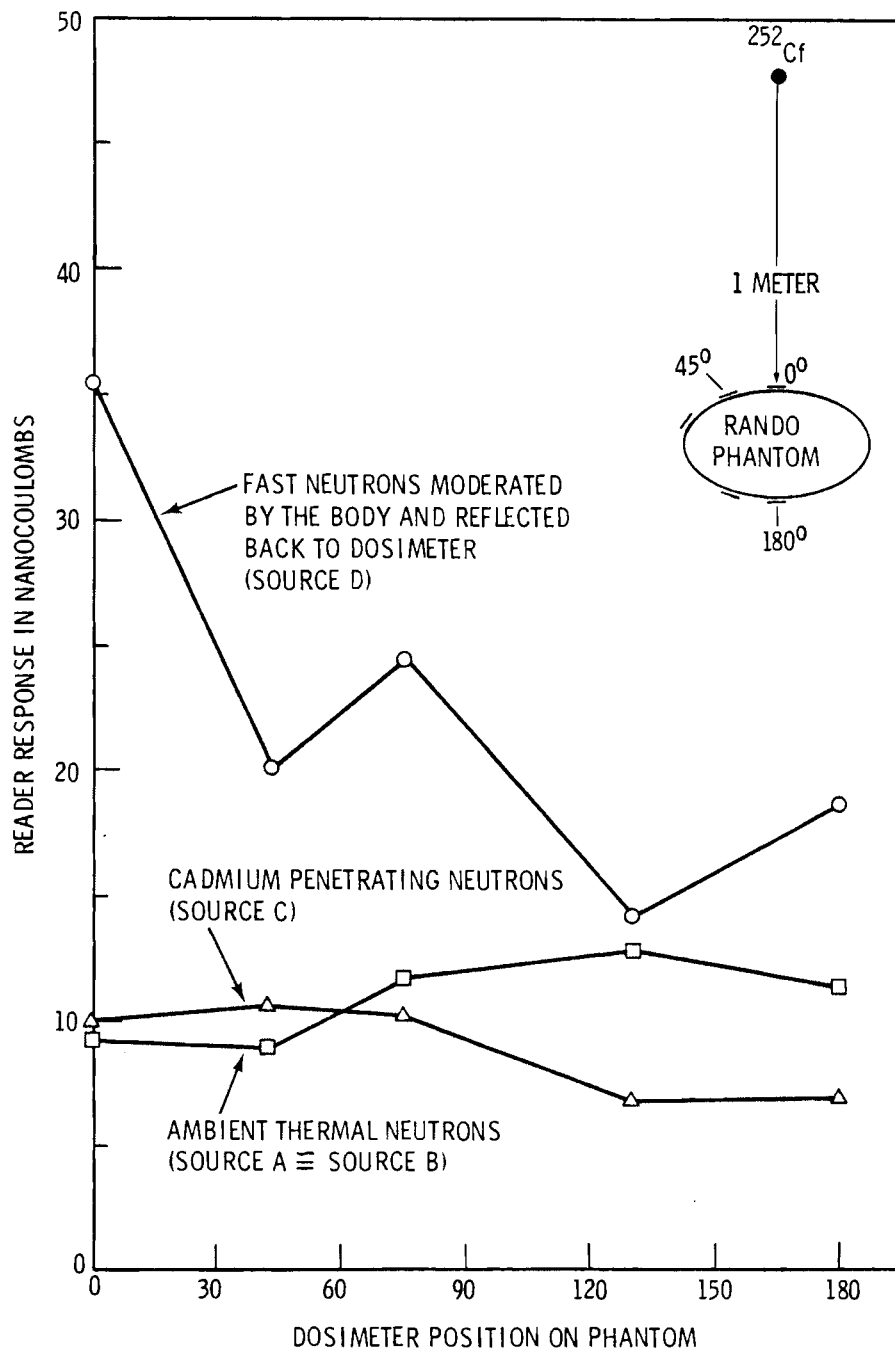


FIGURE 7.4. Components of Neutron Response. (All values are corrected to one meter from source.)

In Figure 7.4, components A, B, and C do not fluctuate greatly with position, whereas component D does fluctuate considerably with position on the phantom. Component D, fast neutrons moderated by the body and reflected back to the dosimeter, is therefore the cause of fluctuation in the readings of chip 3 and 4. Since the dose equation involves  $2R_4 - R_3$ , the fluctuations of D in both  $R_4$  and  $R_3$  are amplified in the calculated fast neutron dose.

There is a depression in component D at approximately  $45^\circ$ . This corresponds to the position just over the lungs of the phantom. This same type of depression over the lungs is shown in Figures 7.3, 7.5, 7.6, 7.9, and 7.10 (these will be discussed later). This depression comes from the lower neutron moderating capability of low-density, lung-equivalent polyethylene just below the surface of the phantom.

#### Effect of Placing a Thin Neutron Moderator Behind the Dosimeter

To further demonstrate that the material immediately behind the dosimeter was the major cause of fluctuating calculated fast neutron dose, a set of HMPDs were exposed on the Rando phantom, identically as shown in Figure 7.3 except that a  $3/8 \times 1-3/4 \times 2-7/16$  inch piece of Plexiglas was attached to the back of each dosimeter as shown in Figure 7.B.1 of Appendix B. This provided a uniform  $3/8$  inch of moderator behind the HMPD. The results are shown in Figure 7.5. Note that the thermoluminescence of chips 3 and 4 changed much more gradually than they did in Figure 7.3. As a result, the calculated fast neutron dose fluctuated considerably less in Figure 7.5 than in Figure 7.3. This demonstrates that the moderator immediately behind the dosimeter is the major source of positional dependence.

Figure 7.5 shows a depression in response in the area over the lungs, as does Figure 7.3 and 7.4. The large deviations from a smooth curve shown in Figure 7.3 have been eliminated by attaching the Plexiglas.

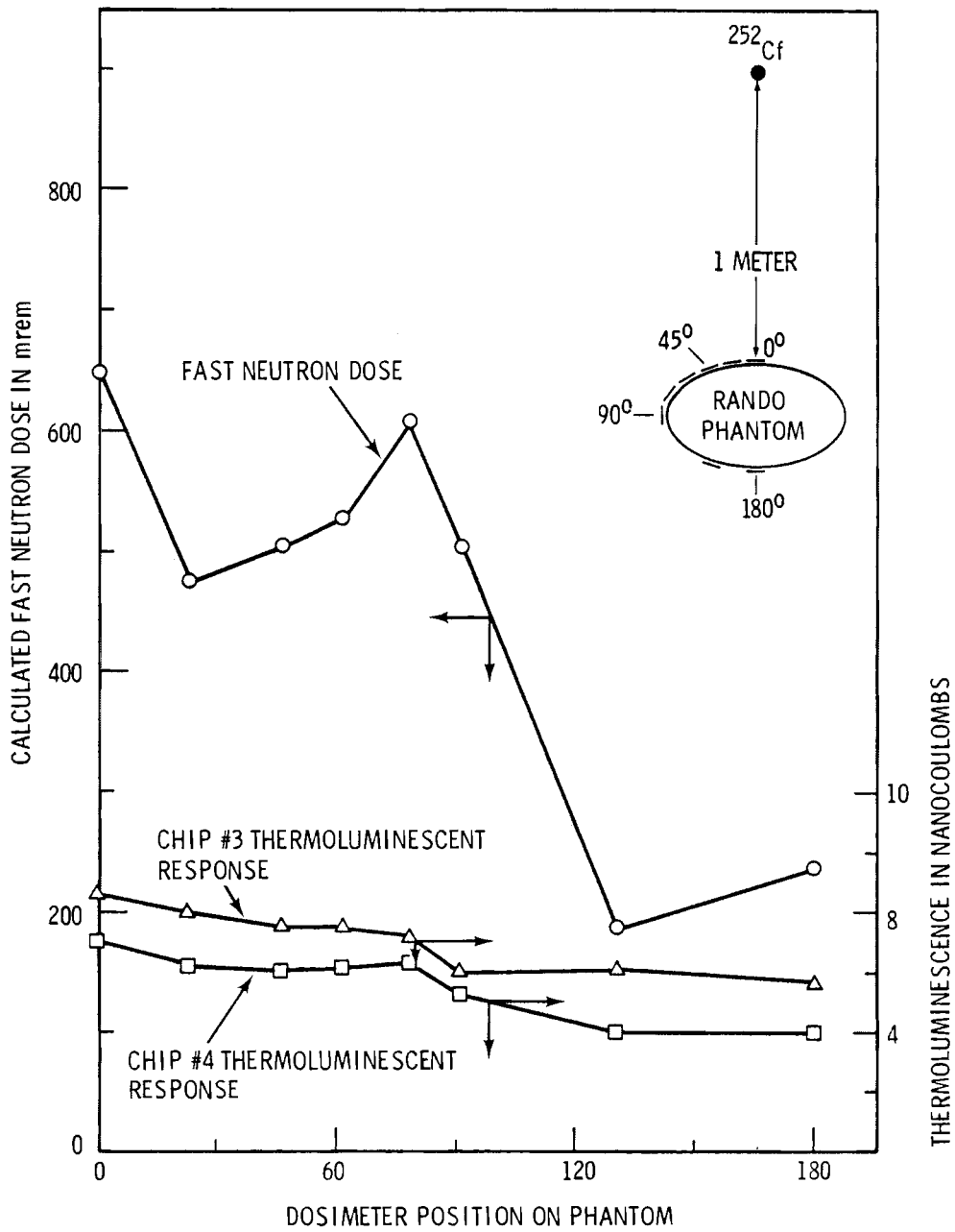


FIGURE 7.5. HMPD Response with 3/8-Inch Plexiglas Between Dosimeter and Rando Phantom. (Dose received is 1000 mrem at front of phantom. All values are corrected to one meter from source.)

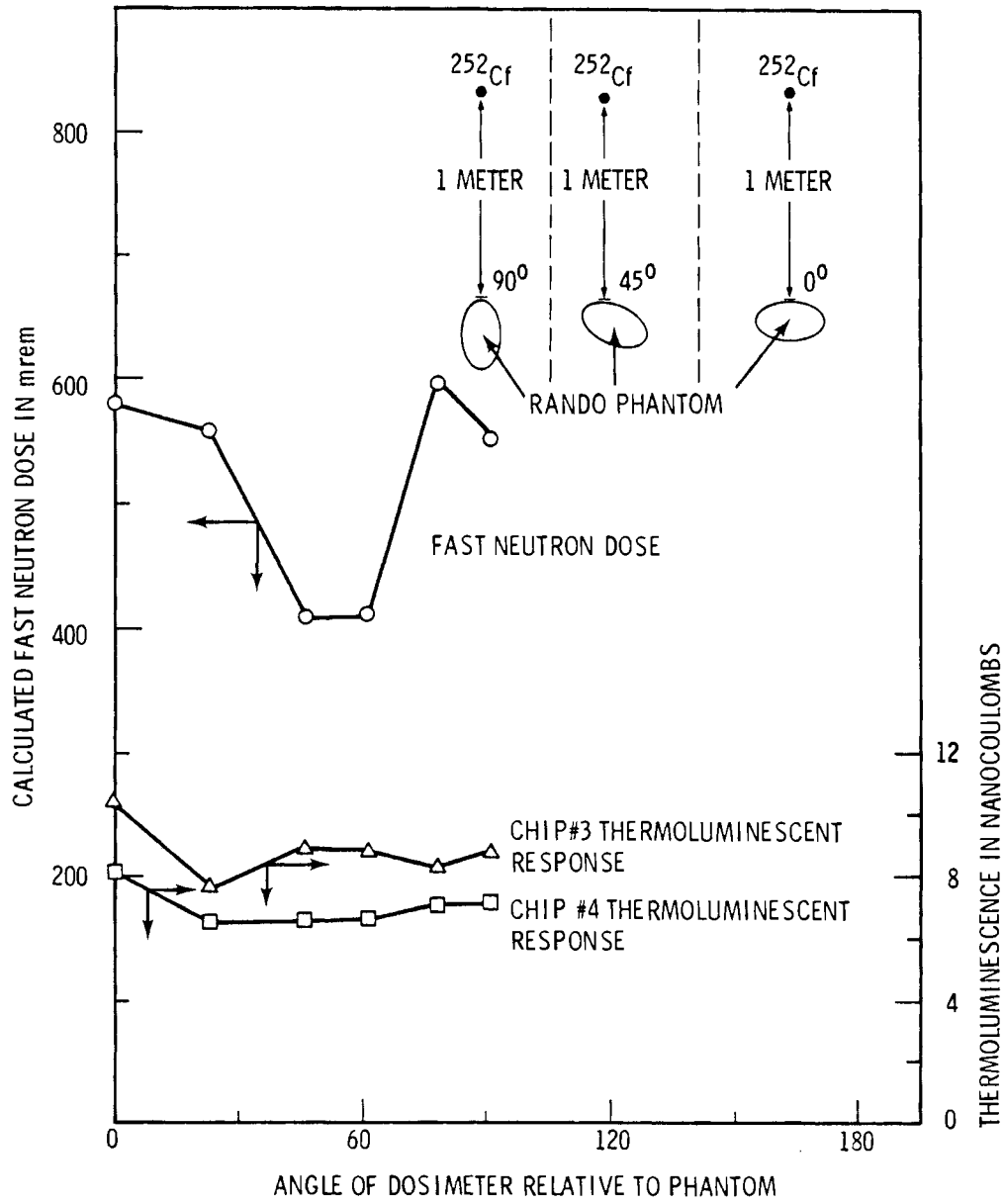


FIGURE 7.6. Rando Phantom Rotated

### Rotating the Rando Phantom

Figure 7.6 shows how the calculated dose varies with position when the dosimeter is one meter from the radiation source and directly faces the source. Since each dosimeter was at the same horizontal level at different positions of the chest region of the Rando phantom, the major factor leading to different calculated fast neutron doses was positional dependence. The positions corresponding to 45° and 60° indicated a fast neutron dose about 30% lower than the other positions at the front of the phantom. The lower calculated dose in these positions was believed to be due to lung equivalent polyethylene just below the surface of the phantom chest. Note that the fluctuations of thermoluminescence of chips 3 and 4 relative to each other was more abrupt in Figure 7.6 for the Rando phantom than the fluctuations in Figure 7.2 for the water jug phantom.

### Quantification of Positional Dependence for $^{252}\text{Cf}$

To quantify the positional dependence of chip 3 and 4's thermoluminescence to  $^{252}\text{Cf}$  fast neutrons the standard deviations for chip 3 and chip 4 in Figure 7.3 and from another set of data were calculated. The other data set came from thermoluminescent data for chips 3 and 4 irradiated as shown in Figure 7.3 except that the  $^{252}\text{Cf}$  source was at 1.5 meter instead of one meter. These standard deviation values were compared to the standard deviations of TLD chips given identical exposures in identical geometries. The difference in standard deviations was assumed to be due to positional dependence.

For values on the Rando phantom, the standard deviations of chips 3 and 4 in percent of total thermoluminescence were 4.02% and 8.81%, respectively.<sup>(a)</sup> For identically exposed TLD chips, their standard deviations were 2.9% and 2.9%. Mathematically the positional dependence for chip 3 (P3) and chip 4 (P4) were calculated as follows:

---

(a) This was based on an average weighted heavily towards the 1.5 meter  $^{252}\text{Cf}$  exposure because this data was less dependent on distance from the source. The standard deviations listed are for the mean reading of two chips because two chips were used behind each filter.

$$\left(\frac{4.02}{100}\right)^2 = \left(\frac{P3}{100}\right)^2 + \left(\frac{2.90}{100}\right)^2$$

$$P3 = 2.78 \%$$

$$\left(\frac{8.81}{100}\right)^2 = \left(\frac{P4}{100}\right)^2 + \left(\frac{2.9}{100}\right)^2$$

$$P4 = 8.32 \%$$

These values were used in Study 8.

#### POSITIONAL DEPENDENCE AS A FUNCTION OF ENERGY

To determine roughly how positional dependence varies as a function of neutron energy, a series of exposures were made on the Van de Graaff accelerator. Five dosimeters were placed on the Rando phantom in the arrangement shown in Figure 7.7. The phantom was placed in a known beam of monoenergetic neutrons and given a known dose. The ratio of dose calculated from HMPD response to dose given was then plotted against neutron beam energy.<sup>(a)</sup>

A linear regression best fit was made for each phantom position to see if the response for each position converged at any energy. This data is shown in Figure 7.8. Lines A, B, C, D, and E correspond to positions A, B, C, D, and E in Figure 7.7.

Although the data was somewhat scattered, the general trend was that the response ratios converged somewhat at energies of 10 MeV and above. At 10 MeV the response ratios between positions differed by about 33% of position D's value. At 100 keV response ratios differed by 54% of position D's value. This means that at neutron energies of 10 MeV and above the placement of the dosimeter was less important than at energies around 100 keV. The magnitude of positional dependence is shown by the ratio between line D and line C to be about 45% greater at 100 keV than it is at 10 MeV.

---

(a) This was drawn on log log paper so the data would lie in a straight line.



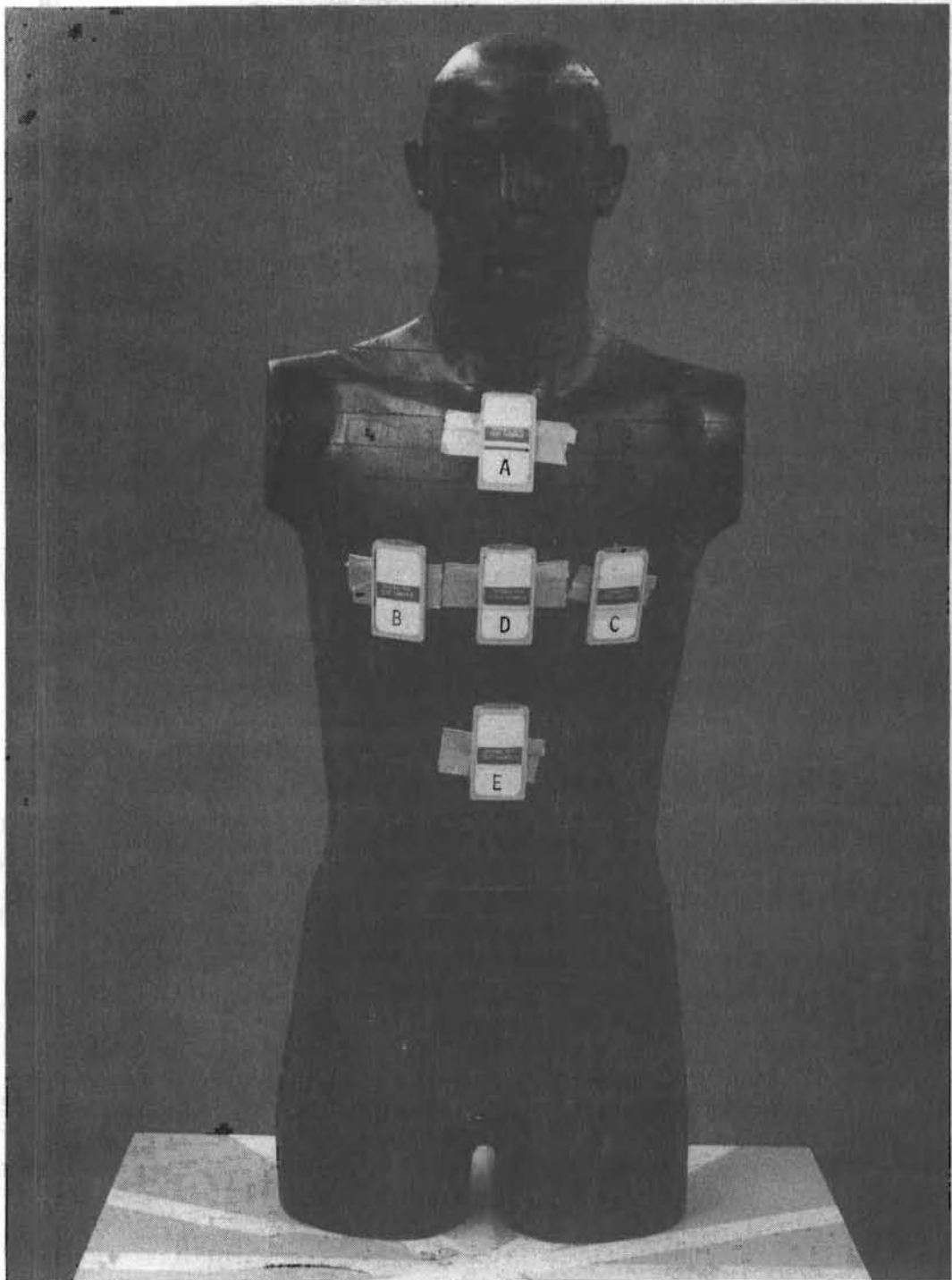


FIGURE 7.7. Dosimeter Placement for Van de Graaff Exposures

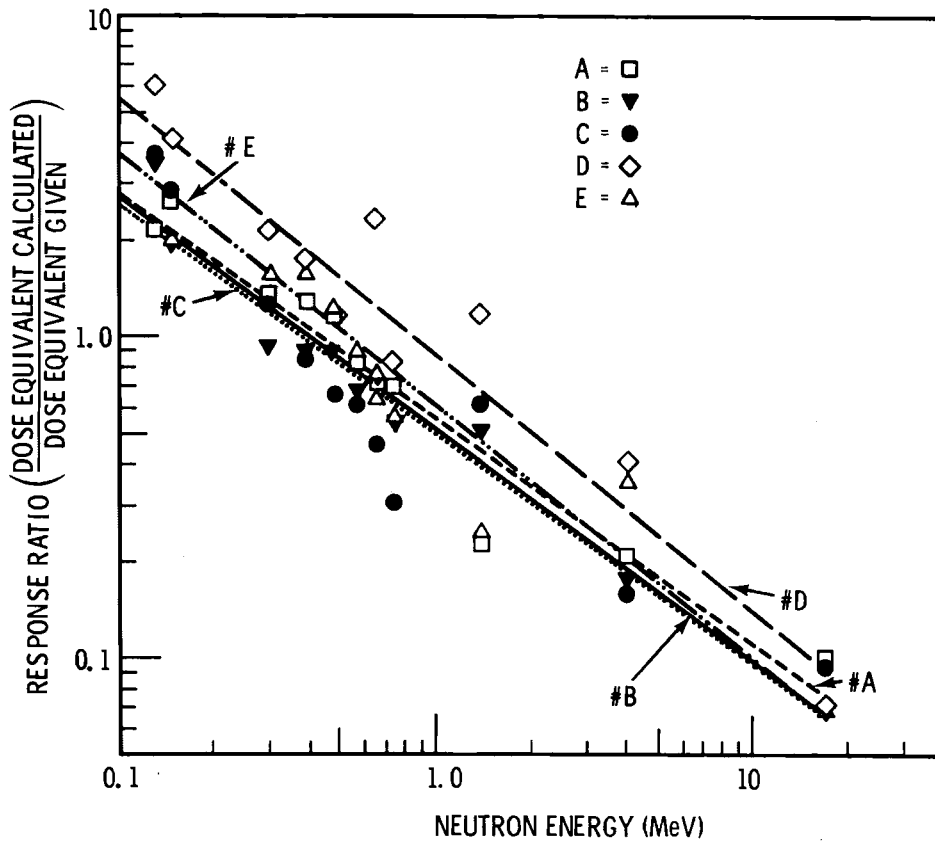


FIGURE 7.8. Positional Dependence as a Function of Energy

The reason why positional dependence (measured by the ratio of D to C) tends to decrease at high neutron energies is because the cross section of hydrogen (the main moderator in both the body and the Rando phantom) decreases at high neutron energies. The cross section of hydrogen is shown in Appendix A. At high neutron energies around 10 MeV, the cross section of hydrogen is about 0.94 barns; whereas, at 100 keV the cross section of hydrogen is 14 barns. In water this corresponds to a 50%-probability path length of 11 cm for 10 MeV neutrons and 0.74 cm for 100 keV neutrons. Since 10 MeV neutrons require more collisions with hydrogen to be thermalized and their mean path length between collisions is greater, the tissue volume which is required to thermalize 10 MeV neutrons is considerably greater than that required to thermalize 100 keV neutrons. The result is that differences in neutron moderating ability of tissue are averaged over a larger volume for 10 MeV

neutrons than 100 keV neutrons. Therefore, the specific placement of the dosimeter is less important for 10 MeV neutrons than for 100 keV neutrons.

#### POSITIONAL DEPENDENCE TO BARE PuBe AND BARE PuF<sub>4</sub>

A series of dosimeters were exposed on the Rando phantom to PuBe and PuF<sub>4</sub> sources to demonstrate positional dependence at two other energies. The average neutron energy of PuBe and PuF<sub>4</sub> is 4.5 and 1.2 MeV, respectively. Their neutron spectrums are shown in Appendix A.

The physical set up used is diagrammed in the upper right corners of Figures 7.9 and 7.10. It was an exposure set up nearly identical to that used for Figure 7.3. The one difference was that a different batch of LiF chips were used for Figures 7.9 and 7.10 than was used for Figure 7.3.

Comparing Figures 7.9 and 7.10, it can be seen that the two curves fluctuated approximately the same amount in percent of calculated fast neutron dose for the front positions (between 0° and 90°). Figure 7.9 shows that the PuBe response had a standard deviation of 19% for the first six positions. Figure 7.10 shows that the PuF<sub>4</sub> response had a standard deviation of 16%. They both fluctuated about the same amount because positional dependence for fast neutrons changes gradually with energy level and their energies differed by only a factor of four.

The calculated dose dropped off considerably from 90° to 180° because the phantom shielded these dosimeters from the neutron source. For the PuF<sub>4</sub> source this was more pronounced than for the PuBe source because the lower energy neutrons of PuF<sub>4</sub> were less able to penetrate through the phantom.

#### ANGULAR DEPENDENCE

To measure dependence of HMPD calculated dose upon angle of the dosimeter relative to the plane of the phantom, a series of exposures were made at the National Bureau of Standards (NBS) and Lawrence Livermore Laboratory (LLL). These exposures involved exposing a water jug phantom to either a neutron beam of known energy at NBS or to <sup>252</sup>Cf at LLL.

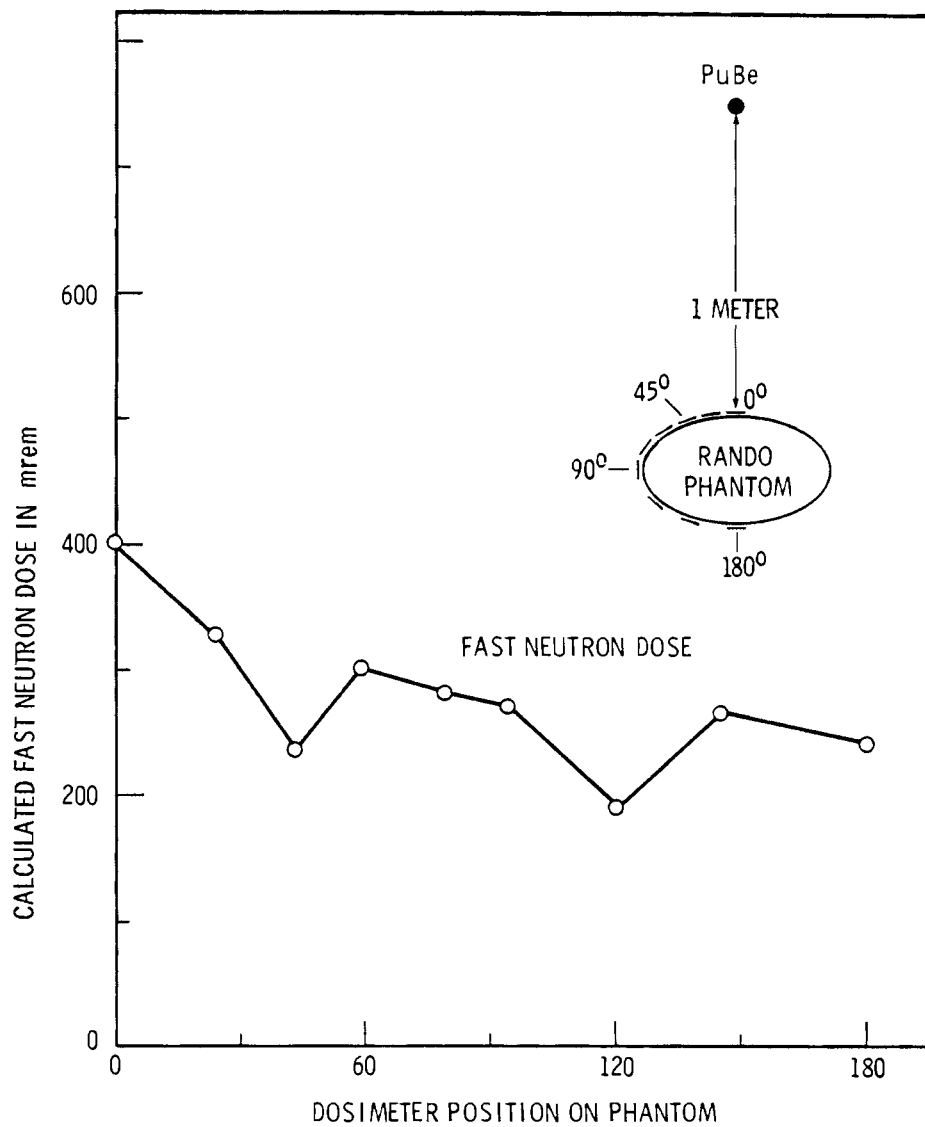


FIGURE 7.9. HMPD Response with Position on the Rando Phantom to PuBe. (Dose is 1000 mrem at front of phantom. All values are corrected to one meter from source.)

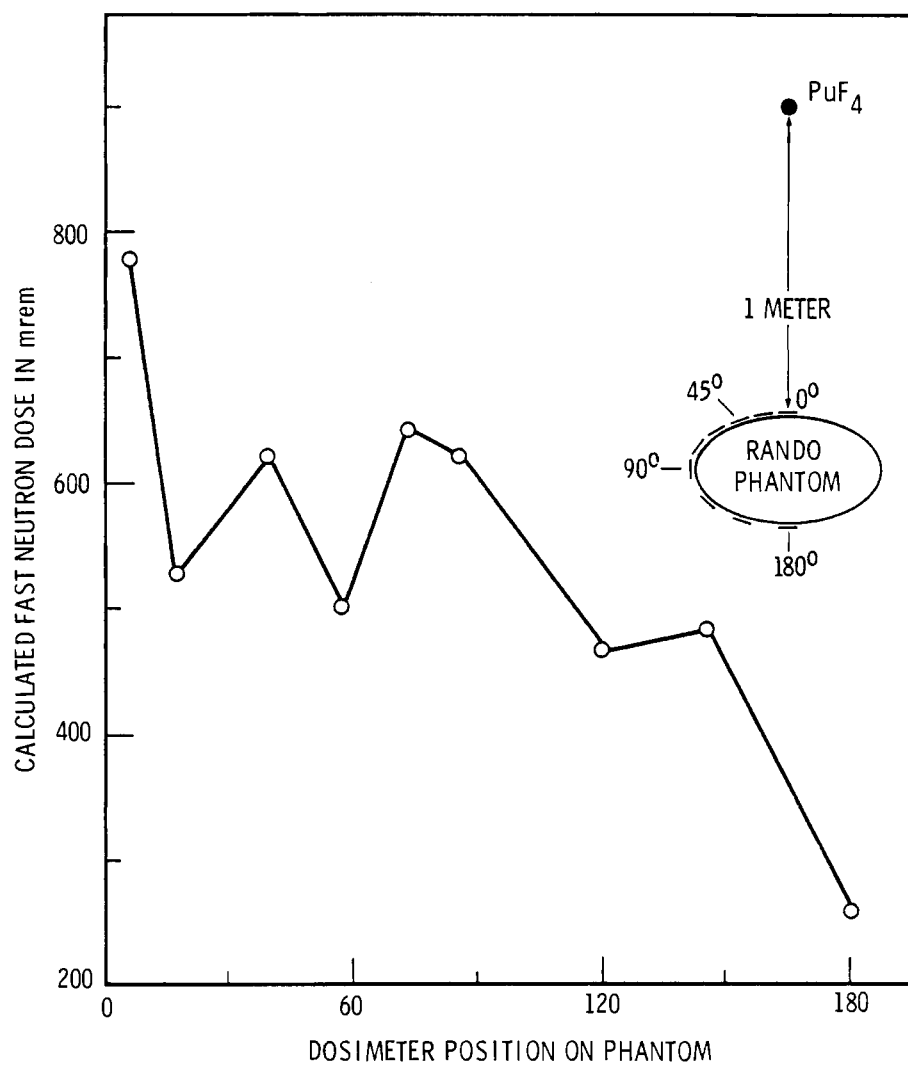


FIGURE 7.10. HMPD Response with Position on the Rando Phantom to  $\text{PuF}_4$ . (Dose is 1000 mrem at front of phantom. All values are corrected to one meter from source.)

The exposure set up and results are shown in Figures 7.11, 7.12, and 7.13.

#### Fast Neutrons

For neutrons above 1 keV, the calculated dose dropped off approximately linearly as the angle was increased from 0° to 45°. At 45° the calculated dose was about 45% of what it was at 0°. Beyond 45°, the calculated dose became a function of room geometry and varied considerably from exposure to exposure. These data are shown in Figures 7.11 and 7.12.

#### Thermal Neutrons

For thermal neutrons in Figure 7.13, the response decreased less than 10% as the angle between the plane of the dosimeter and plane of the phantom was increased from 0° to 45°. Beyond 45°, the calculated thermal neutron dose dropped off dramatically to only 27% to that of the 0° exposure.

#### RESPONSE DEPENDENCE WITH DISTANCE SEPARATING PHANTOM AND DOSIMETER

The response of the HMPD to fast neutrons as the dosimeter is held directly in front of the Rando phantom is shown in Figure 7.14. For these exposures, the plane of the dosimeters and phantom were parallel and the dosimeters were spaced from the phantom by hollow cardboard inserts.

As the distance between the dosimeter and phantom increased, the "field of view" occupied by the phantom decreased leading to the decrease in thermoluminescence of chip 3 and 4. Somewhat counteracting this, the shadowing effect of the cadmium filter on chip 4 was reduced as the distance between the dosimeter and phantom increased. When the dosimeter was spaced 2.3 cm from the phantom, the calculated fast neutron dose was only 78% of that when the dosimeter rested flat on the phantom.

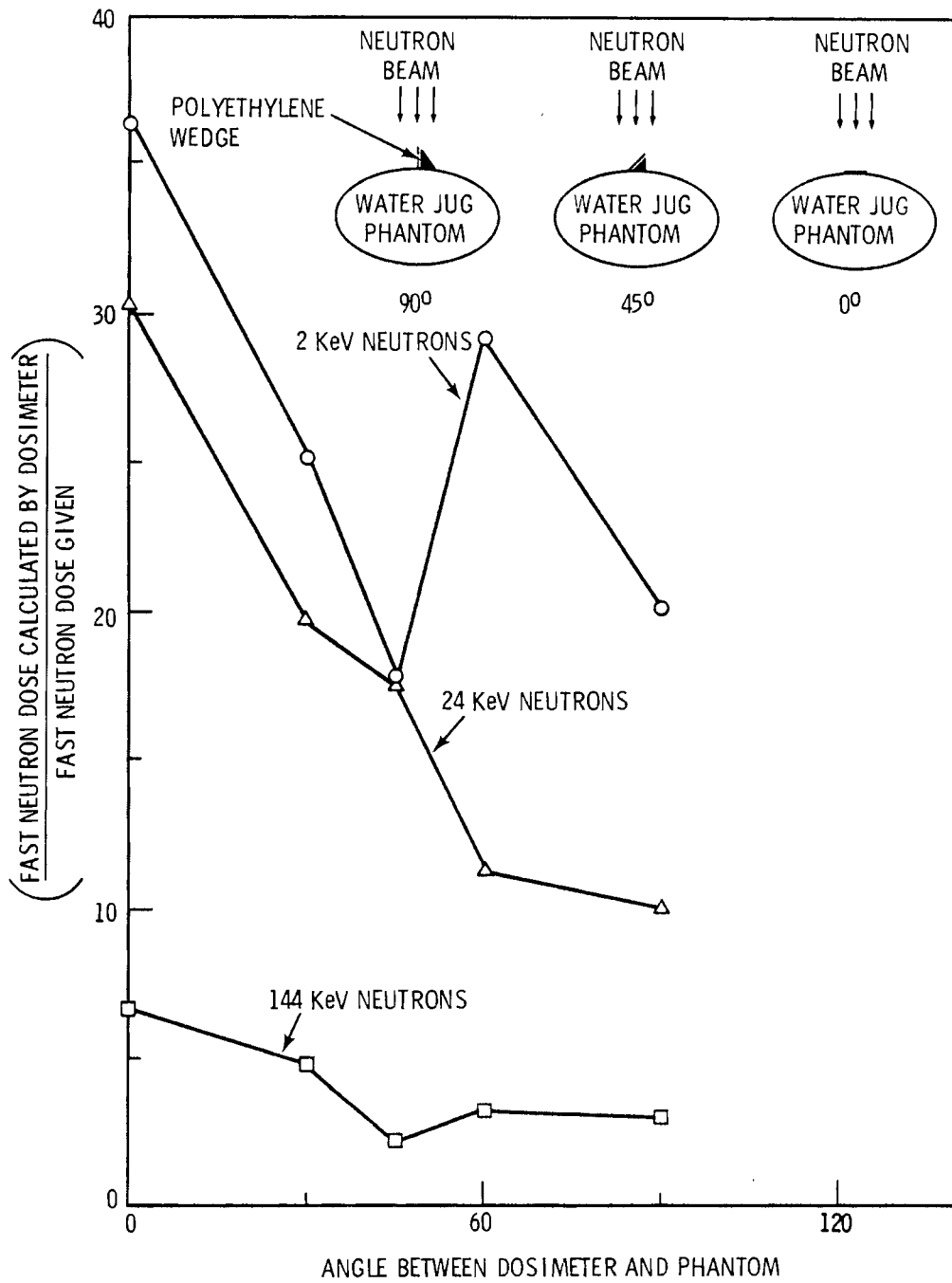


FIGURE 7.11. HMPD Response to Fast Neutrons as a Function of Angle Between Dosimeter and Phantom.

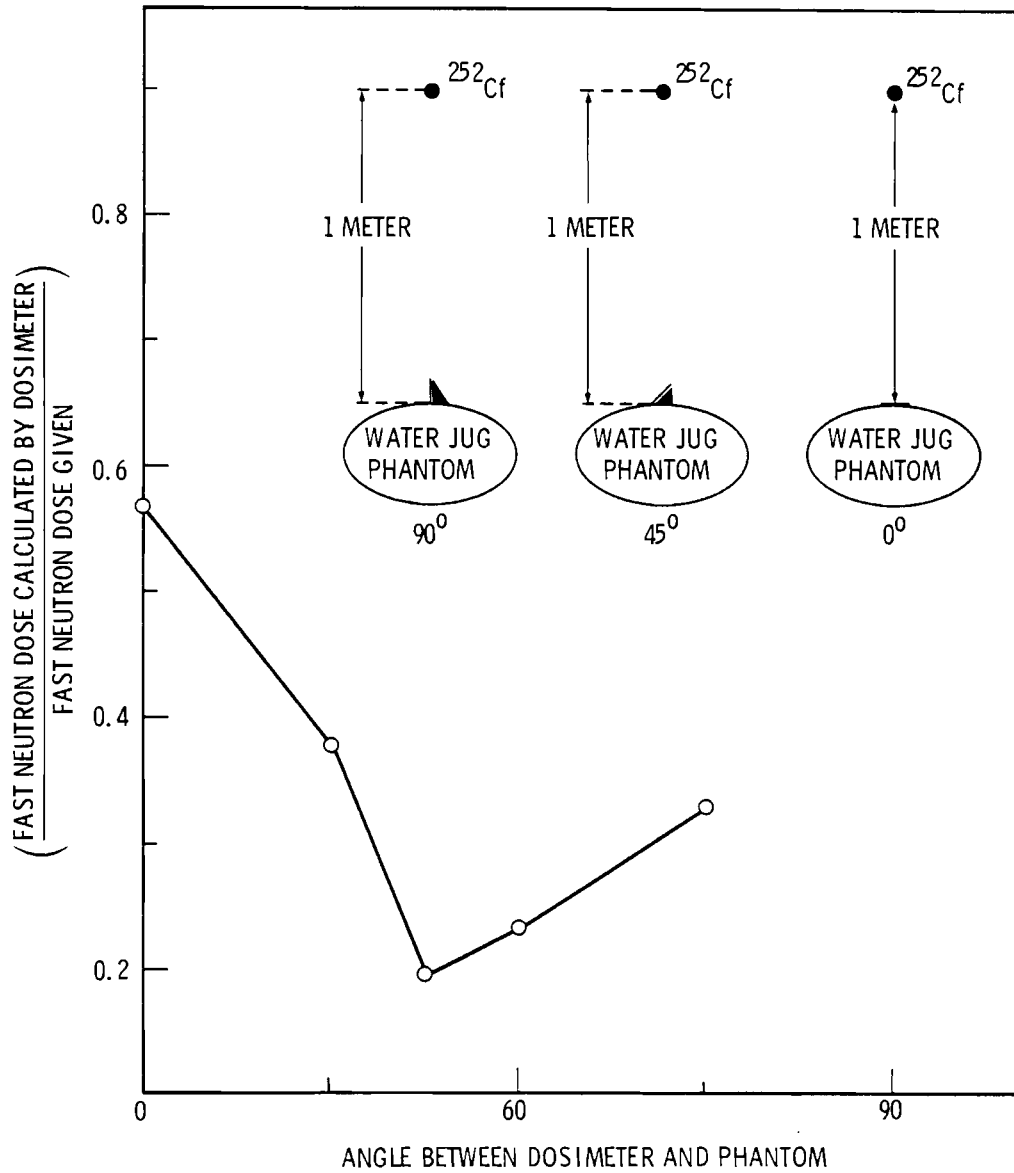


FIGURE 7.12. HMPD Response to  $^{252}\text{Cf}$  as a Function of Angle Between Dosimeter and Phantom.



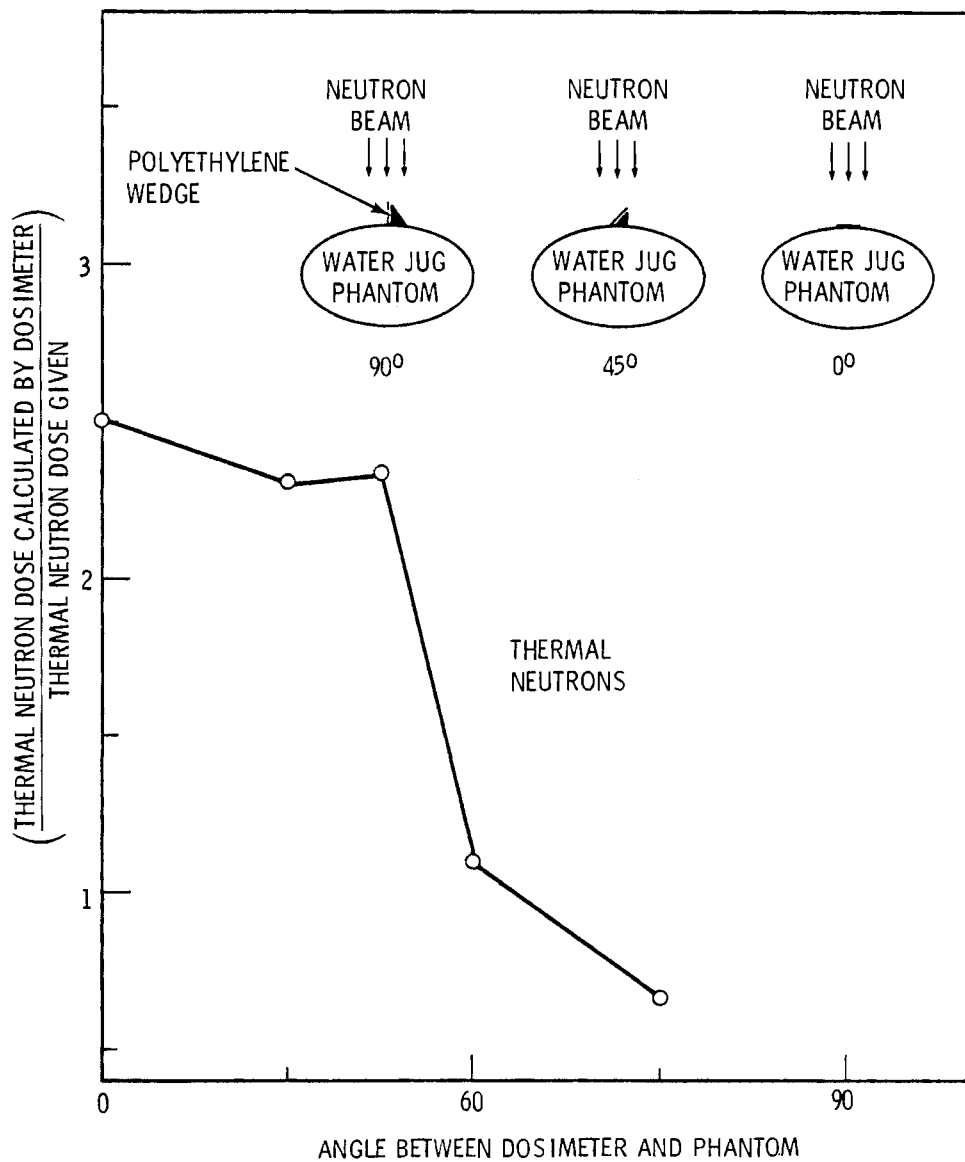


FIGURE 7.13. HMPD Response to Thermal Neutron As a Function of Angle Between Dosimeter and Phantom.

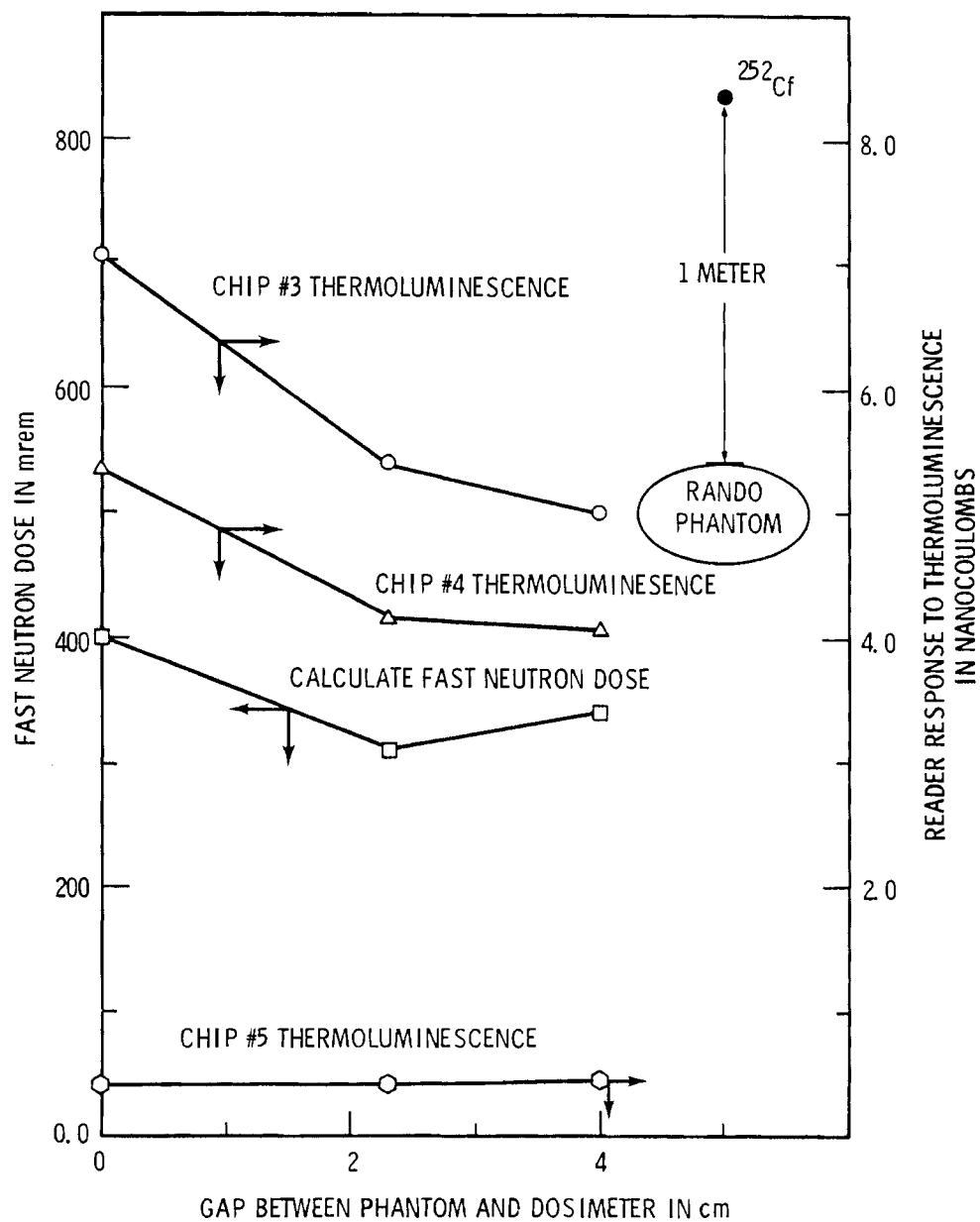


FIGURE 7.14. Response to  $^{252}\text{Cf}$  as a Function of Distance Between Phantom and Dosimeter.